Available online at www.eccomasproceedia.org
Eccomas Proceedia COMPDYN (2021) 3059-3072

ECCOMAS
Proceedia

COMPDYN 2021
8th ECCOMAS Thematic Conference on
Computational Methods in Structural Dynamics and Earthquake Engineering
M. Papadrakakis, M. Fragiadakis (eds.)
Streamed from Athens, Greece, 28 - 30 June 2021

SEISMIC FRAGILITY ASSESSMENT FOR A CLASS OF RC SCHOOL BUILDINGS IN ITALY LEVERAGING DETAILED AND REDUCED-ORDER MODELS

Sergio Ruggieri[1], Giuseppina Uva[1]

[1] Polytechnic University of Bari
Via Amendola, 70126 Bari, Italy
{sergio.ruggieri, giuseppina.uva}@poliba.it

Abstract

A study is presented on the seismic fragility analysis of a class of existing RC school buildings in Puglia, Southern Italy. Firstly, we defined a taxonomy for identifying a homogenous building class, through the collection of typological data, such as construction age, number of storeys and construction materials. After, by means of the available Census data on Italian school buildings, we selected 735 units in the focused area to assembly a proper database to involve in the phase of numerical modelling and analysis. To assess fragility, we employed two modelling options: (a) a single-degree-of-freedom approach, by evaluating the backbone of the simplified models; (b) a multi-degree-of-freedom approach, by means of some index buildings of the class for which a full knowledge of geometrical and mechanical properties is available, as well as their spatial nonlinear numerical models. Nonlinear time history analyses were performed on all simplified models to define specific class fragility, accounting for any source of variability (record-to-record and building-to-building). The results of the investigation are compared in terms of class fragility curves, in order to highlight the differences between the two modelling approaches.

Keywords: Class Fragility Curves, Typological Data, SDOF Models, MDOF Models.

ISSN:2623-3347
Peer-review under responsibility of the organizing committee of COMPDYN 2021.
doi: 10.7712/120121.8696.18784

1. INTRODUCTION

The studies about seismic fragility at class-level of buildings have recently become increasingly numerous among researchers, which try to individuate the main sources of vulnerability and to reduce the related risk of several typologies of building portfolios. Of growing interest are the investigations focused on the existing building stock, which is often characterized by an high probability of damage, especially if subjected to earthquakes. Several examples of the catastrophic effects given by earthquakes are available, with regard to different building typologies having different social importance, such as residential [1-2], strategic (e.g., schools [3-4] or hospital), precast and ecclesiastical buildings [5]. A myriads of approaches can be employed for defining fragility functions for class-level assessment purposes, in which four macro-categories can be identified: (i) empirical [6-7], (ii) mechanical [8-11], (iii) judgemental [12] and (iv) hybrids methods. Among these, in this study we are going to argue about mechanical ones, focusing on the results achievable by different modelling approaches.

Generally, the mechanical methods allow to perform fragility/vulnerability assessment through a direct derivation of the relationship between seismic intensity and damage states/losses. This is possible by means of the analysis results (usually nonlinear dynamic or static) carried out on numerical models, which simulate a single or a class of buildings. The results of a fragility function, elaborated for large-scale purpose, is strictly related to the quantity and the quality of the numerical models at disposal, which in turn depends from the available data. With this regard, Silva et al. [13] defined the two extreme options: (a) few detailed multi-degree-of-freedom (MDOF) models; (b) many single-degree-of-freedom (SDOF) models. The first option consists in the selection of few real (or idealized) archetypes representative of a certain building class, characterized by a detailed knowledge of all structural components and all geometrical and mechanical properties. This is the case of the so-called index-buildings, which are usually selected through the expert opinions of the analyst, as made in [10,14]. Obviously, an incorrect selection of the index-building properties can lead to a misleading fragility evaluation, frustrating the related analysis efforts. The second option consists in an extensive analysis process on a large number of reduced-order models, generated on the base of few data and outlined through simple computations. The easy management and the evident discount in terms of analysis efforts makes the SDOF models the most attractive option, as shown in several literature works [15-16], although the loss of accuracy in each single model (e.g. local responses, structural irregularities) assumes a key role in the fragility estimate. In the middle, other methods are available from the scientific literature, balancing accuracy vs. complexity and quantity vs. quality of numerical models [17-19].

In all cases, by referring to class-level fragility, the starting point is the definition of a building taxonomy, which can vary on the basis of the sample size. As a matter of fact, to represent the overall fragility of a specific class via simple SDOF models, few data are necessary, such as the construction material, the year of construction or the number of storeys. On the other hand, the adoption of complex MDOF models requires the knowledge of detailed information, which implies a not always sustainable economic and computational burden in the investigation and analysis phases.

Anyway, the goodness of the fragility function is strongly influenced by two not negligible aspects: (a) the analysis method (b) the uncertainty treatment. On the analysis side, static pushover (SPO) analysis [20] and nonlinear response history analysis (NRHA) contend for the title of best, where the first approach wins in simplicity and intuitiveness, while the second approach dominates the first one in the prediction of seismic response of buildings, accounting for the real nature of earthquakes (use of ground motions) and for the features variability of any kind of buildings (e.g., structural irregularities, influence of higher modes). On the uncertainty side, NRHA approach can be preferred in class-fragility analysis, where record-to-record variability can be taken into account by evaluating its contribute on the basis of the number of records employed, the selected intensity measure (IM) and the investigated engineering demand parameter (EDP). In addition to this kind of uncertainty, the intra-building and the inter-building uncertainties are to consider, where the first one refers to the uncertainty in the knowledge of each investigated building and the second one aims to define the variability of each building in the selected ensemble to represent the class.

In this wide range of options, a study on the fragility function of a class of real school buildings in Puglia (Southern Italy) is provided, by exploring the two abovementioned modelling extremes: many simple SDOF models vs. few complex MDOF models. Given a building taxonomy, the comparison among fragility curves at safety limit-states is provided, by using the results of 10 complex MDOF models selected from the work by Ruggieri et al. [21] and the response of 735 SDOF models elaborated from the information contained in some freely available exposure databases (ISTAT Census data [22], ARISTOTELES Project [23], Open Data about Italian schools provided by Italian Ministry of University and Research (MIUR) [24]). Fragility functions will be developed by opting for a NRHA approach, as well as by running cloud analyses on MDOF models and incremental dynamic analyses (IDAs) on SDOF models [25]. For the case at hand, we can anticipate that the seismic behaviour of SDOF models (e.g., backbone curve), which could be evaluated through any number of methods proposed by the scientific literature, has been evaluated looking at the MDOF models, their modelling assumptions and their seismic response.

2. MODELLING METHODOLOGIES FOR SDOF SYSTEMS FOR CLASS-LEVEL ASSESSMENT POURPOSES

The use of SDOF models for developing class fragility/vulnerability functions has been often adopted by researchers to limit the computational burden for larger sets of buildings [15-16]. The parametrization of the inelastic behaviour of SDOF, as well as the backbone shape, can be elaborated through different fairly popular procedures. For example, Ruiz-García and Miranda [26] elaborated a probabilistic approach to estimate the maximum inelastic displacement demands of SDOF systems, by providing a new version of the R-μ-T (strength ratio-ductility-period) relationship [27], trough the definition of the constant-strength inelastic displacement ratios. Vamvatsikos and Cornell [28] proposed a pushover-based approach to investigate the dynamic behaviour of SDOF models, simulated through a quadri-linear backbone and contextually, authors developed the SPO2IDA tool. The same approach was involved in the analytical studies developed in FEMA P440A [29], which presents the force-displacement capacity of some spring typologies to employ in SDOF systems for simulating different building behaviours, expressed in terms of maximum inter-story drift ratio (θ_{max}) vs. the normalized base shear on the yield value ($V_b/V_{b,y}$ or F/F_y). Lagomarsino and Giovinazzi [30], proposed the relationships to relate macro-seismic and mechanical-based approaches, in which authors provided criteria to trace the SDOF backbone curves for several class of European buildings. Vamvatsikos and Aschheim [31] adopted the paradigm of Performance-Based Design, by means of Yielding Frequency Spectra approach, to define an equivalent SDOF model from a MDOF one, as well as after applied by Kohrangi et al. [32] in the vulnerability model for buildings in the municipality of Isfahan, Iran.

Herein, we are adopting the procedure suggested in [32], by assuming a backbone curve of SDOF models (and the boundary control points for the spring to employ, in terms of θ_{max} vs. F/F_y) according to the seismic behaviour of full MDOF models, given a building taxonomy. With regard to the building taxonomy, it is necessary that both SDOF and MDOF models are belonging to same class, which is defined by the parametrization of at least five parameters, usually available in freely online databases: construction typology (CT), year of construction (CY), number of storeys (NS) and two values among in-plan area (A), total volume (V), interstorey height (H_i) and total height (H_{TOT}). Within the online databases containing the required information, the parameters A and V are often available and they can be employed by means of simple equations and assumptions, to estimate all the key features of the building taxonomy. In particular, knowing CT, CY and NS, the other parameters can be find with the following equations (or with the inverse formulations):

$$H_{TOT} = \frac{V}{A} \tag{1}$$

$$H_i = \frac{H_{TOT}}{NS} \tag{2}$$

In addition, assuming the typical values of gravity loads (L) for the selected building class, it is possible to compute the total mass (M) and the total weight (W) of the buildings:

$$L = G + \psi_{k2} \cdot Q_k \tag{3}$$

$$W = A \cdot L \cdot NS \tag{4}$$

$$M = \frac{W}{g};\ m_i = \frac{M}{NS} \tag{5}$$

where G and Q are, respectively, the dead and the accident loads, ψ_{k2} is the combination coefficient for the quasi-permanent k^{th} load, g is the gravity acceleration and m_i is the mass of the i^{th} storey. While Q can be defined on the basis of the prescriptions provided by the current building code, G is an unknown parameter, which can be established on the basis of the typical features of the building typology investigated. To support the definition of G, the knowledge of the technologies and the loads detected on some MDOF buildings is fundamental, in order to identify the most employed typologies of slabs, external and internal masonry infills, floor tiles and other finishes.

To define the SDOF behaviour, the formulation defined in [31] and developed in [32] can be employed, where the parameters of an equivalent SDOF are provided. In particular, given the building taxonomy, the approach consists in the definition of eight parameters and a SDOF backbone shape. Among the eight parameters, NS and H_i are directly identified from the input building database. Three of the eight parameters can be fixed a-priori, as well as the participation factor (Γ) and the mass participation factor (a_1) for the first vibration mode and the conventional damping ratio (ξ). For the case at hand, both Γ and a_1 can be fixed equal to 1, as suggested in [32]. The remaining three parameters are:

- The base shear coefficient, C_y, identified as the ratio between the yield base shear and the total weight of the structure ($V_{b,y}/W$);
- The yield storey drift, θ_y, evaluated on the real elastic behaviour of MDOF building;
- The coefficient of distortion, α_{COD}, which represents the ratio between the peak interstorey drift and the related roof drift, as following defined:

$$\alpha_{COD} = \frac{\theta_{max}}{\theta_R} \tag{6}$$

Operationally, C_y can be defined on the yield code spectrum given the yield displacement (δ_y), because it is equivalent to yield spectral acceleration (expressed in unit of g). To define δ_y as suggested in [31], the following equation can be adopted:

$$\delta_y = \frac{\theta_y \cdot (NS \cdot H_i)}{\Gamma \cdot \alpha_{COD}} \tag{7}$$

Eq. 7 depends from the parameters θ_y and α_{COD}, where the first one can be defined by observing the behaviour of the available MDOF structures, while α_{COD} can be defined according to [33, 34]. This parameter is the simpler way to define the deformation behaviour of buildings and, for a generic MDOF system, α_{COD} ranges between 1.1 and 1.4 as long as the building behaves as elastic. After the yielding and for higher values of θ_{max}, α_{COD} tends to increase, as shown in [31]. For a one-storey building α_{COD} is equal to 1. Once that all the eight parameters are defined, the period of each SDOF system (T^*) can be evaluated as:

$$T^* = 2\pi \cdot \sqrt{\frac{\delta_y}{C_y \cdot g}} \tag{8}$$

Finally, to define the backbone shape of SDOF system, it is possible to purse different options, basing on the expected behaviour of the simulated buildings. The simpler option is the elastic-plastic shape, while to better simulate the post-elastic behaviour it is possible to refer to the parametric capacity curve shapes provided by FEMA-P440A [29]. The presented SDOF models can be employed in the fragility function, by means of the results provided by the analysis phase. Some additional remarks can be added for the development of the procedure. Firstly, for a class-level purpose, different seismic actions can be considered within the focused area and the definition of the yield spectral acceleration can be differentiated on the basis of the buildings localization. After, some of the eight parameters, such as θ_y, can be established a-priori on the basis of the CY of the buildings and the reference building code [32]. Nevertheless, the detailed knowledge of the structural behavior of some MDOF structures, representative of the building class, can be used for having a reliable indication about the effective values to employ in the procedure. In the end, also the adoption of the FEMA-P440A backbone curves [29] could represent a simplification. Also for this aspect, the seismic response of few MDOF structures belonging to the identified class can be employed for a calibration of a specific-class backbone curve shape, to involve in the fragility function through the simplified modelling approach.

3. DEFINITION OF AN HOMOGENEUS CLASS OF SCHOOL BUILDINGS IN PUGLIA, SOUTHERN ITALY

The starting point of this study is represented by 15 real RC school buildings in the province of Foggia, Puglia, Southern Italy. In particular, for these buildings, which present a generalized in plan irregularity, a near-full information of the geometrical and mechanical features is available and, according to the work by Ruggieri et al. [21], the 3D numerical models of buildings and the related pushover analyses in both directions are at disposal. Following the procedure in Section 2, within this sample of buildings, it is possible to define an homogenous subset aimed to identify a building taxonomy, according to some key parameters and additional historical information.

Firstly, all buildings present a *NS* ranging from 2 to 3, which suggest that the entire sample is constituted by low-rise buildings, also according to the classification provided by HAZUS [35]. After, concerning to the *CT*, all buildings are RC moment-frame buildings, which do not present RC walls and all buildings present infill panels (in some cases, the eternal frames are totally infilled, while in others they are partially infilled and presenting ribbon windows). The discriminant parameter is the *CY*. Despite all buildings were designed between 60' and 80', three main historical aspects have to be considered to define the building taxonomy [23]:

- After some modifications occurred in 1935 and in 1969, the Apulian seismic map was upgraded in 1981, and some municipalities of the Province of Foggia (North of the Region) were redefined from non-seismic to low-seismic areas, as shown in Figure 1.
- Between 1972 and 1979, Italian governments released a new version of the Italian building code, in which new design rules were introduced accounting for the first anti-seismic requirements.
- In the subsequent years to the Second World War (from 1945 to 1950), new buildings difficultly presented RC moment-frame structural systems, because it was very likely the

presence of masonry structural parts. This evidence was caused by the aftermaths of the Fascism that previously forbade the use of the steel in Italy.

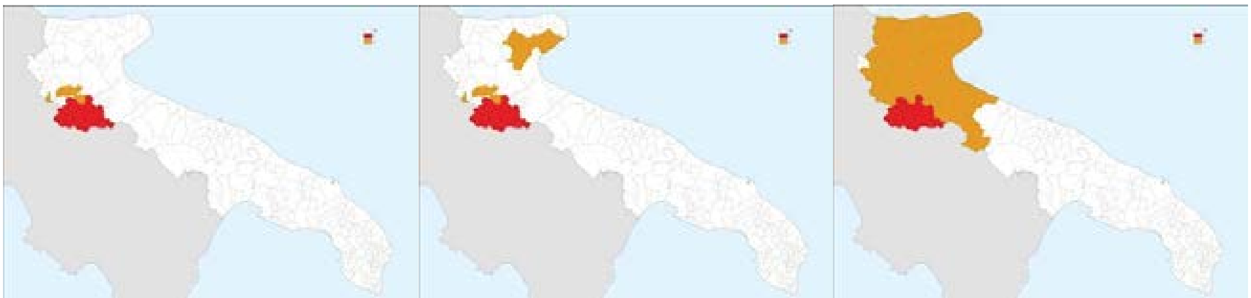

Figure 1 – Evolution of the seismic classification in Apulian Region with reference to, respectively, 1935/03/25, 1962/11/25 and 1981/3/7 [23]. The white part indicates non-seismic areas, the orange part indicates a low-seismic areas (zone 2) and the red part indicates a medium-high seismic areas (zone 1)

Then, with regard to *CY*, the buildings belonging to homogenous class are the ones built between the 1950 and 1979 and located in the municipalities classified as non-seismic areas (according to the seismic classification provided by Italian governments and shown in Figure 1), within the indicated time period. According to the identified building taxonomy, 10 of 15 school buildings fall under the homogenous class. Figure 2 reports the pushover curves in both main directions (X and Y, according to the reference system adopted in [21]) for the new subset of buildings, labelled as B1-B10 (From the total sample, B3, B4, B5, B6 and B10, as defined in [21], have been excluded and the remaining 10 buildings have been renumbered).

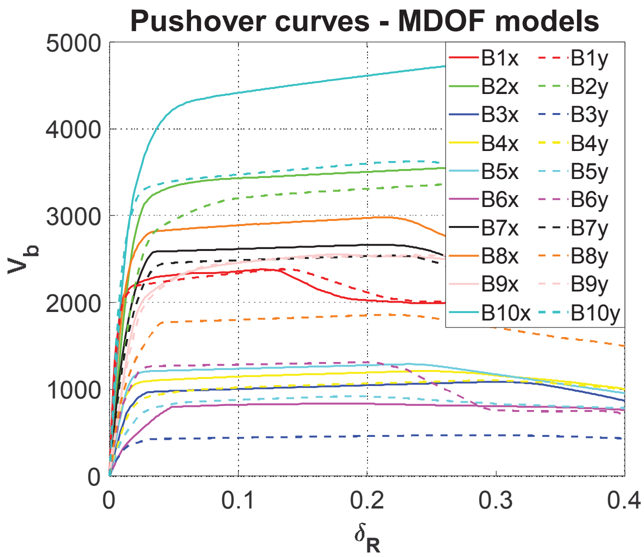

Figure 2 – Pushover curves in both directions (X,Y) of the 10 RC school buildings, belonging to the identified building class

For a purpose of class-level assessment, given the building taxonomy, several buildings can be identified from freely available databases, for which few data are at disposal. For the case at hand, two open databases have been consulted and elaborated: (a) database developed in ARISTOTELES Project [23] and (b) Open Data about Italian schools provided by Italian Ministry of University and Research (MIUR) [24]. From the first database, which was based on the ISTAT Census data [22], information about all the existing schools in Puglia have been gathered with reference to 2001. In particular, data on *CY*, *CT*, *NS*, *V*, *A*, municipalities where buildings are located and the related seismic evolution in the time were extracted. From the second database, information about all the existing schools in Italy have been collected with reference to 2019. In detail, it presents only the exact location of each school building (municipality, address, postal code) and information on *CY*, *A* and *V*. In both databases, each unit presents an univocal code to identify the school. By matching the two databases through the comparison of the common data (univocal code, municipality, *CY*, *A* and *V*, evaluated with a certain tolerance) and with regard to the given building taxonomy, 735 existing RC school buildings have been selected. All data have been elaborated according to the Eqs. 1-5. More in detail, after the evaluation of H_i and H_{TOT} for all buildings, a value of L equal to 6 kN/m^2 has been supposed, given by the assumption of a value of G equal to 5 kN/m^2, a unique value of Q_k equal to 3 kN/m^2 and a value of ψ_{k2} equal to 0.3 in accordance with the Italian Building code (NTC18) [36]. Figure 3 reports the geographical distribution of all identified buildings, where the greater part of the units are located in the South and in the Central of the Region, while only few buildings have been considered in the North, accounting for the existing seismic zoning in the assumed time interval.

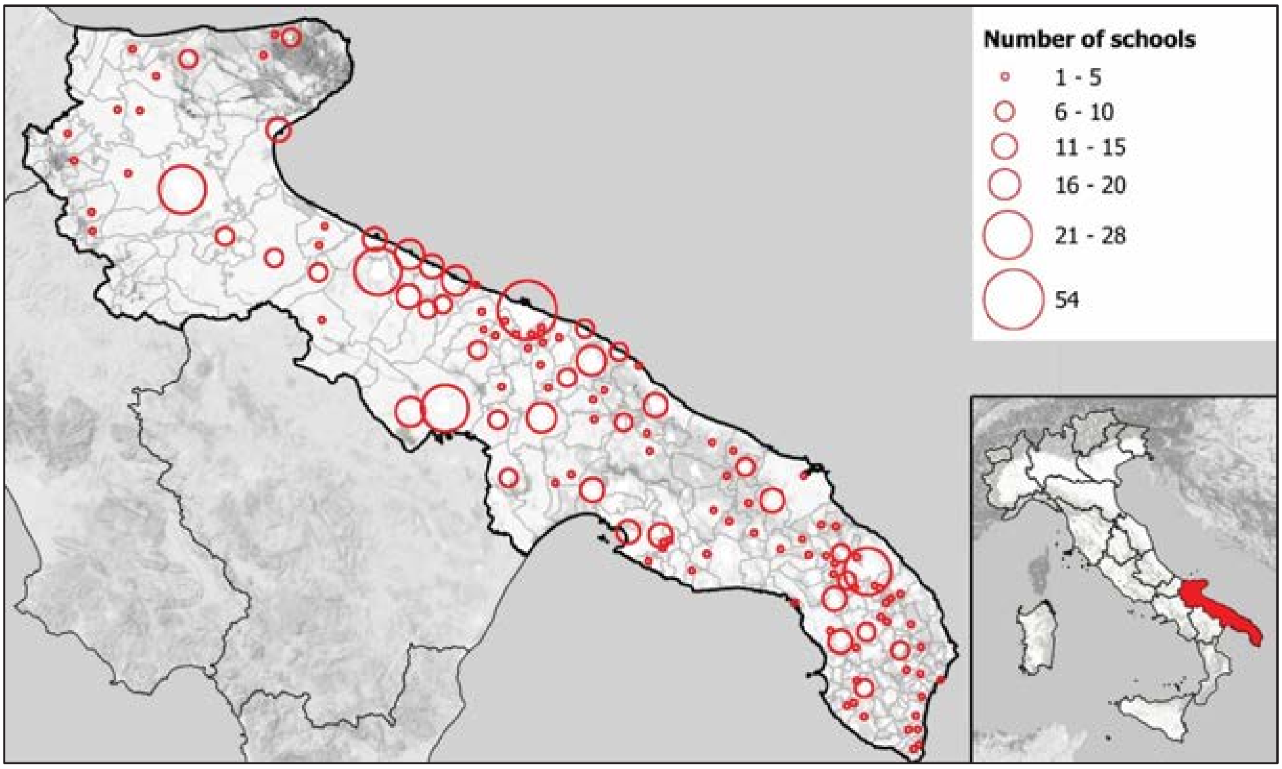

Figure 3 – Distribution of the selected 735 school buildings along the Region, according to the given taxonomy

4. SEISMIC FRAGILITY ASSESSMENT AT CLASS-LEVEL

4.1 Numerical models

For both samples made by 10 MDOF and 735 SDOF systems, different modelling strategies have been employed. Concerning to the modelling of the 10 full models of the known school buildings, the reference is the work made in Ruggieri et al. [21], where the nonlinear MDOF models were carried out through a lumped plasticity approach and by implementing all the geometrical and mechanical features at disposal. As just shown in Figure 2, a ductile behaviour is assumed, by neglecting for simplicity the influence of shear mechanisms and infill panels. Nevertheless, as declared in [21], shear failures given by low transversal reinforcement of structural elements can be evaluated a posteriori, by checking the brittle mechanisms of beams and columns. After, all the 735 buildings belonging to the homogenous class have been elaborated for a SDOF approach. More in detail, looking at the SPO curves of the 10 MDOF structures, a value of θ_y equal to 0.25% has been fixed while, according to [32], the values of α_{COD} are assumed equal to 1, 1.25 and 1.35, respectively for 1-storey, 2-storeys and 3-storeys buildings. Using Eq. 7, the values of δ_y have been defined for all buildings. Later, assuming an elastic code spectrum, the values of C_y have been defined, which are the same values of the spectral accelerations. Finally, by means of Eq. 8, the values of T^* have been determined. With regard to the assumed elastic code spectrum, the seismic actions in the regional capital (Bari, which is in the Central of the Bari) has been considered, as good compromise between the higher seismicity in the North and the lower seismicity in the South. Still, in the elastic code spectrum has been computed by using an unitary behavior factor and by considering an usage class adequate to school buildings, with a coefficient equal to 1.5. Lastly, no any amplification factors due to e.g., soil and topography categories have been considered. For few cases of the buildings investigated, high values of V_{by} are obtained, considering high values of A, as typical for school buildings in the focused geographic zone. In addition, a large set of T^* is identifiable, which ranges about from 0.3 s to 0.8 s and given by the different NS that characterize buildings in the considered sample.

Therefore, all 735 buildings have been modelled through nonlinear SDOFs oscillators. In particular, the springs of the SDOF systems have been simulated by using OpenSees software [37], opting for a Pinching4 material to define the quadri-linear force-displacement capacity boundaries. Regarding to the backbone capacity of the springs employed in the SDOF models, "spring 3b" provided by FEMA-P440A [29] has been considered. As a matter of fact, according to the modelling strategy adopted for the MDOF structures, a ductile behaviour has been accounted for, as visible in the backbone curve shape reported in Figure 4 (right), which also reports the boundary control points of the backbone curve. All coordinates of the normalized hinge (each point is indicated with a letter, labelled from A to G) are specified in Table 1 and they are reported in terms of θ_{max} vs. F/F_y. In conclusion, the results about SDOF models are displayed in Figure 4 (left), where capacity curves of 735 models are displayed in terms of C_y and δ_R^* (light grey lines) as well as the mean and the standard deviation of all realizations (black lines).

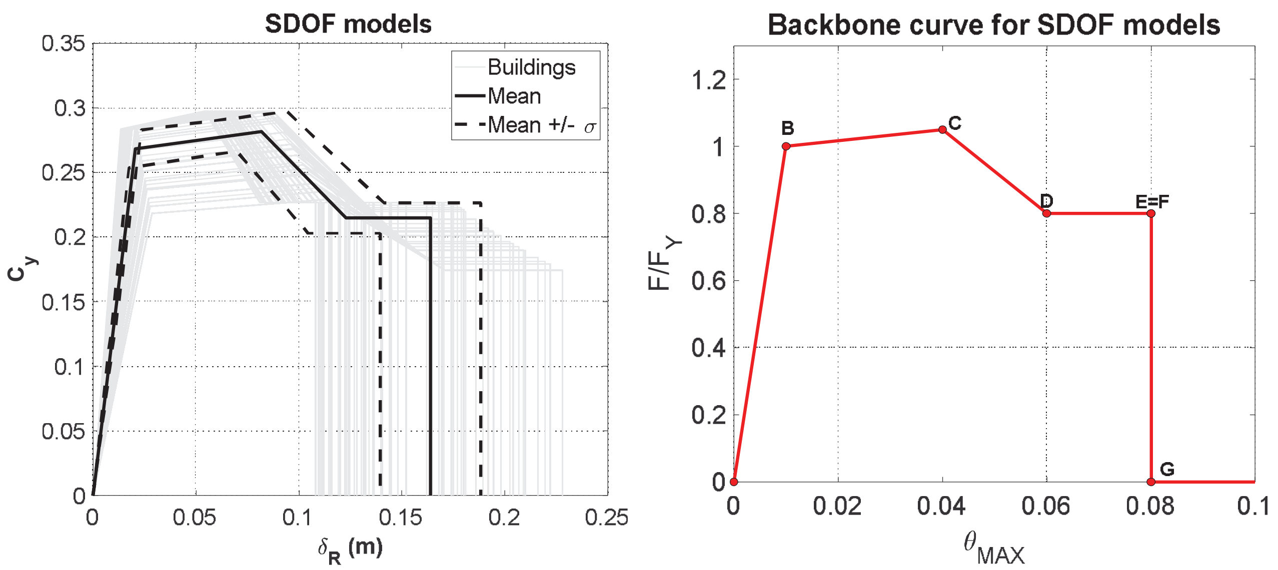

Figure 4 – Capacity curves of the 735 SDOF models generated, displaying mean and standard deviation (left); Backbone curve of SDOF models, according to the prescriptions provided by FEMA-P440A [29] (right)

Table 1. Coordinates of the boundary control points of the Spring "3b" by FEMA-P440A [29], expressed in terms of F/F_y vs. θ_{max}

Structural system	Quantity	B	C	D	E	F	G
Spring 3b - FEMA-P440A [29]	F/F_y	1.00	1.05	0.80	0.80	0.80	0.00
	θ_{max}	0.01	0.04	0.06	0.08	0.08	0.08

4.2 Seismic analysis and class fragility function

The structural response of the 735 SDOF models have been investigated through NRHAs, according to the IDA methodology, while the MDOF models were investigated through SPOs analyses and NRHAs [21]. These latter analyses were performed according to a practice-oriented principle (computational cost reduction) and, for this reason, only few NRHAs have been carried out. With regard to the number of records employed, MDOF models were subjected to a set of 11 ground motion records characterized by two horizontal components, to investigate 3D models in both main directions. For sake of comparison, the same set of 11 ground motion records has been employed herein, by running IDAs with all the 22 horizontal components to each SDOF model. Figure 5 shows an example of the analyses performed on the numerical models, both for SDOF and MDOF systems, by assuming as IM the average spectral acceleration (*AvgSa*) evaluated in a range period from 0.2 s to 2 s and as EDP, the values of θ_{max}. In particular, IDAs on the SDOF model n. 10 are shown in the left graph while cloud analyses on B1 are shown in the right graph, where black and red dots indicate, respectively, non-collapsed and collapsed points (Both models are characterized by a *NS* equal to 2). Regarding to the cloud analyses on 3D models, the results have been recorded in both main directions and, for sake of comparison they are expressed in an unique IM-EDP plane, by considering as response the square-root-of-sum-of-squares rule of the θ_{max} in both main directions. Having the structural responses for both sets of models, fragility analysis have been performed. In particular, the fragility functions are differently developed for the two modelling extremes. For identifying the EDP distribution conditioned by the IM value, a power law approximation has been developed on the structural responses of MDOF systems [38], while an IM-basis approach has been employed to IDA results of SDOF systems.

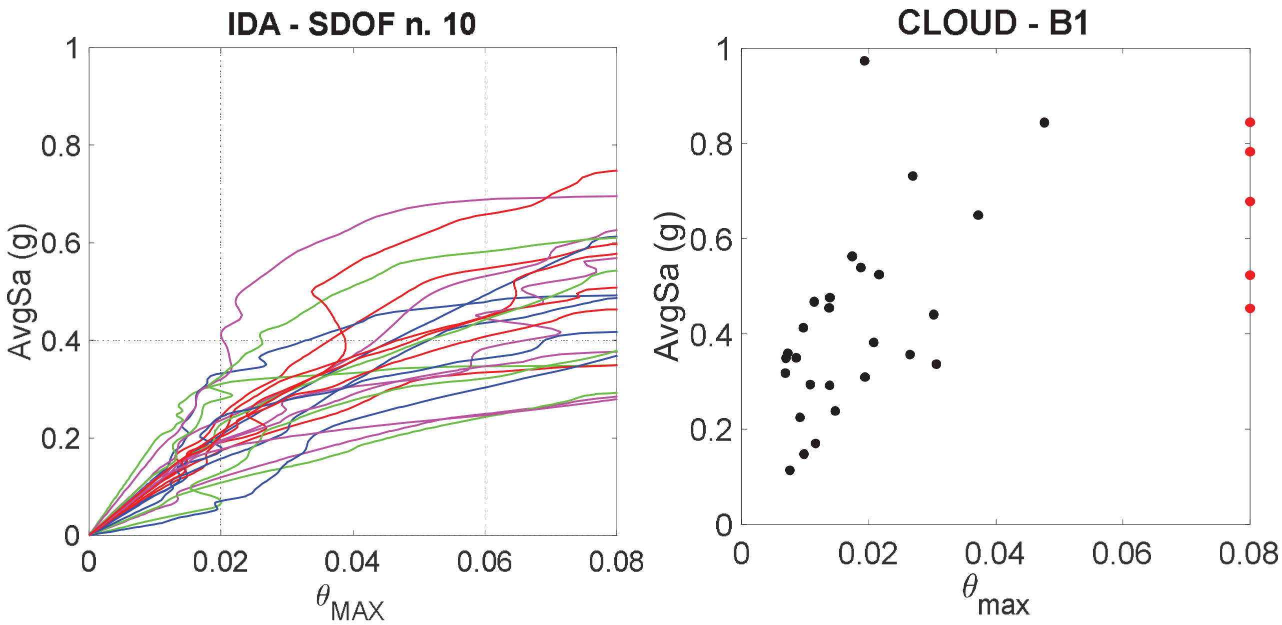

Figure 5 – IDAs on SDOF models (plot for SDOF model n. 50) vs. cloud analysis on MDOF model (plot for building B1, where black and red dots indicate, respectively, non-collapsed and collapsed points)

With regard to the limit-states to investigate, in this study all evaluations have been referred to the safety limit-states, considering that the collapse mechanisms can be given by brittle and ductile failures. In a practice-oriented view, three limit-states have been defines, as well as near-collapse (NC) for brittle and ductile mechanisms and life-safety (LS) for ductile mechanisms. While the achievement of the limit-states can be evaluated independently on each MDOF system by observing the effective structural behaviour of the simulated buildings, a different approach needs to be employed for SDOF models. As a matter of fact, despite a large sample of SDOF models allows to provide a good coverage of all buildings falling into the entire class, this modelling approach does not guarantee an accurate structural failures prediction, especially in the cases of structural irregularities and of higher modes relevance. To establish a valid approach that combines the effective local and global behaviours provided by MDOF models and the simplified estimates provided by SDOF models, fixed values of θ_{max} have been assumed for both the involved modelling approaches. In particular, a θ_{max} equal to 0.5% has been assumed for NC-brittle limit-state, while thresholds equal to 3.2% and 4.3% have been assumed, respectively, for LS- and NC-ductile limit-states.

These limits are selected by extending the mean values of the thresholds obtained for the buildings selected from the work by Ruggieri et al. [21] to the overall behaviour of the backbone curves for SDOF models. Looking at the boundary control points in the backbone capacity curve (Figure 4, right), NC ductile limit-state is fixed on the branch *C-D*, which identifies the softening part that leads to the residual lateral strength, while LS is fixed in the branch *B-C*, precisely at the end of the hardening phase.

Once that fragility curves have been evaluated for all units of the identified class, accounting for all limit-states of interest (NC - brittle, LS and NC - ductile) and for the two modelling and analysis approaches (cloud on 10 MDOF vs. IDAs on 735 SDOF), class fragilities are estimated by virtue of the laws of total expectation and total variance. In particular, the ensemble lognormal mean (μ_C) is given by the mean of all individual lognormal means, while the related dispersions (β_C) are evaluated through the sum of the squares of the intra-building and inter-building dispersions. The class fragility curves are displayed in Figure 6, in terms of probability of exceedance of the building capacity conditioned by the IM value assumed for the limit-state considered ($P[IM > IM_C \mid IM]$, where IM_C is the capacity IM), both for the 735 SDOF models (left, with all fragility curves for all individual units, displayed in light grey) and the 10 MDOF models (right). Table 2 reports the values of the fragility curves parameters, in terms of μ_C and β_C.

The comparison among the two modelling options shows that for the NC-brittle limit-state, the values of μ_C and β_C are similar while for the LS-ductile and NC-ductile limit-states, the values of μ_C and β_C obtained by SDOF models are lower than the ones provided by MDOF models. Nevertheless, considering the percentage difference obtained in terms of μ_C for NC-brittle limit state, which is in the order of 50%, it is evident how the two modelling approaches do not return comparable results. This is mainly due to the structural irregularity presented by MDOF structures (and by school buildings in general), which cannot be predicted by a simple SDOF modelling approach. As a matter of fact, as shown in Figure 5, the results obtained by SDOF models are conservative, also for lower values of θ_{max} and for an elastic behaviour, which should return similar values of μ_C for a fixed EDP value. These disparities in results lead to improve the simplified modelling approaches for fragility analysis at class-level, especially for irregular buildings. Other reasons can justify the obtained differences, considering that the higher dispersions of the fragility curves obtained by the MDOF models can be addressed to the combination of some aspects: (i) few models are available for representing the class; (ii) few NRHAs have been performed on MDOF structures; (iii) the continuous IM-EDP representation through power law is characterized by a certain approximation degree. Obviously, the choice of running few NRHAs on MDOF models allow to reduce the computational cost related to the analysis, which represents a limit in a large-scale analysis. On the SDOF approach side, the main advantage of the approach is the possibility to consider the differences in median responses of the sample (inter-building dispersion) and the structural responses given by the set of records employed (intra-building dispersion). On the other hand, the knowledge of the structural behaviour of some MDOF structures could play a key role in the SDOF system definition, because it could allow to better fix some parameters, e.g. backbone curve shape, limit-state thresholds, besides to account for the structural irregularities. In the end, the proposed comparison shows advantages and disadvantages of the two modelling and analysis extremes in the seismic fragility prediction at class-level, with different results that require further investigations, especially for the SDOF modelling.

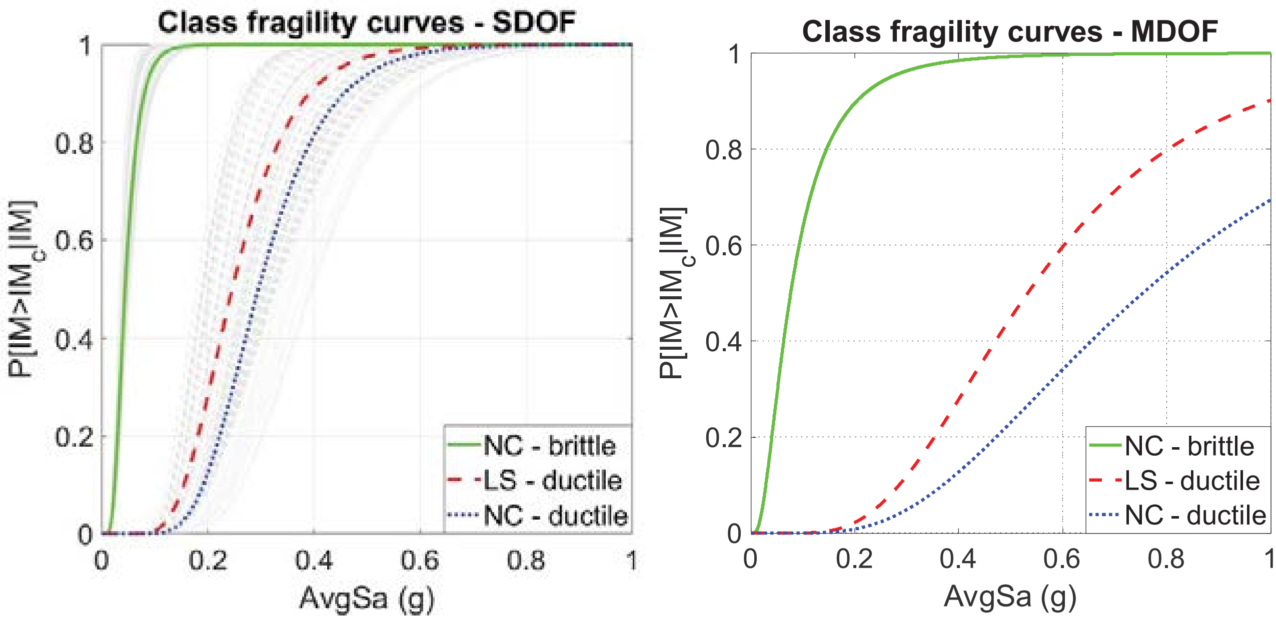

Figure 6 – Fragility curves for the specific-class investigated, accounting for safety limit-states (NC - brittle, LS and NC - ductile) and for the two modelling approaches (SDOF and MDOF)

Table 2. μ_C and β_C values for fragility curves of the specific-class investigated, accounting for safety limit-states (NC - brittle, LS and NC - ductile) and for the two modelling approaches (SDOF and MDOF)

Model	NC (Brittle)		LS (Ductile)		NC (Ductile)	
	μ_C	β_C	μ_C	β_C	μ_C	β_C
SDOFs	0.045	0.466	0.246	0.340	0.296	0.362
MDOFs	0.077	0.763	0.533	0.488	0.753	0.557

5. CONCLUSION

A study on the seismic fragility of existing RC school buildings in Southern Italy is presented, by leveraging on few detailed MDOF models and a large sample of simplified SDOF models. In the first step, a building taxonomy for the specific-class has been investigated, by defining the ranges of some typological parameters, such as the construction typology, the year of construction and the building height. After, by using the available data from some freely databases containing information about Italian school buildings and based on the Census data, 735 buildings have been selected and a SDOF modelling approach has been employed. The lateral behaviour of the 735 models has been defined on the basis of methodology developed in [31, 32], and they have been compared with 10 buildings belonging to the class, for which a full modelling and the nonlinear analyses results are available [21]. The entire sample of 735 reduced-order models have been generated and investigated through IDAs. The comparison among the safety fragility curves obtained by the two modelling approaches, the two analysis methods and the two samples of buildings having a different size, provides different results for safety limit-states, as well as brittle and ductile ones. The differences confirm the evidence that the SDOF modelling herein adopted is low accurate to predict the behaviour of irregular buildings, also for low EDP values, which imply an elastic behaviour of buildings. Generally, conservative estimates are provided by SDOF models, with higher values of medians and dispersions for MDOF models. From the MDOF side, the choice of index buildings that effectively represents the class is the main hurdle, as well as the complexity and the effort for an extensive analysis phase. On the other hand, MDOF system represents the best way to reproduce the seismic response of the class, accounting for global and local behaviour. From the SDOF side, the methodology allows to consider a more accurate estimate of the structural responses for the given building class, accounting for any source of variability (record-to-record and building-to-building). In the end, the characterization of the simple models could require the knowledge of the overall behaviour of more complex structures belonging to the class, which drives to find future calibration processes, especially for irregular structures as school buildings. The employment of the two modelling extremes in class fragility studies and subjected to different nonlinear analyses suggests advantages and disadvantages of both methodologies, as well as the necessity to further investigations to improve the approaches at class-level.

ACKNOWLEGMENTS

Authors thank Prof. Dr. Dimitrios Vamvatsikos for his kind help and insightful suggestions in the development of the work. The research presented in this article was funded by the Italian Department of Civil Protection in the framework of the national project DPC-ReLUIS 2019-2021.

REFERENCES

[1] Zuccaro, G., Perelli, F. L., De Gregorio, D., & Cacace, F. (2020). Empirical vulnerability curves for Italian masonry buildings: evolution of vulnerability model from the DPM to curves as a function of acceleration. Bulletin of Earthquake Engineering, 1-21.

[2] Del Gaudio, C., Di Ludovico, M., Polese, M., Manfredi, G., Prota, A., Ricci, P., & Verderame, G. M. (2020). Seismic fragility for Italian RC buildings based on damage data of the last 50 years. Bulletin of Earthquake Engineering, 18(5), 2023-2059.

[3] Di Ludovico, M., Digrisolo, A., Moroni, C. et al. (2018) Remarks on damage and response of school buildings after the Central Italy earthquake sequence. Bull Earthquake Eng. https://doi.org/10.1007/s10518-018-0332-x

[4] Ruggieri S., Tosto C., Perrone D., Uva G., Aiello M. A. (2021) Assessment of post-earthquake damages on Italian school building portfolios over the last 50 years. In COMPDYN 2021, 8th ECCOMAS Thematic Conference on Computational Methods in Structural Dynamics and Earthquake Engineering.

[5] Ruggieri, S., Tosto, C., Rosati, G., Uva, G., & Ferro, G. A. (2020). Seismic Vulnerability Analysis of Masonry Churches in Piemonte after 2003 Valle Scrivia Earthquake: Post-event Screening and Situation 17 Years Later. International Journal of Architectural Heritage, 1-29.

[6] Rossetto, T. and Elnashai, A. (2003) Derivation of Vulnerability Functions for European-Type RC Structures Based on Observational Data. Journal of Engineering Structures, 25, 1241-1263.

[7] Rota, M., Penna, A. and Strobbia, C. L. (2008) Processing Italian damage data to derive typological fragility curves. Soil Dynamics and Earthquake Engineering , 28(10-11), 933-947.

[8] Aiello, M. A., Ciampoli, P. L., Fiore, A., Perrone, D., Uva, G. (2017) Influence of infilled frames on seismic vulnerability assessment of recurrent building typologies. Ingegneria Sismica, 34(4), 58-80.

[9] Ruggieri, S., Porco, F. & Uva, G. (2020) A practical approach for estimating the floor deformability in existing RC buildings: evaluation of the effects in the structural response and seismic fragility. Bull Earthquake Eng 18, 2083–2113. https://doi.org/10.1007/s10518-019-00774-2

[10] Vamvatsikos, D., Bakalis, K., Kohrangi, M., Pyrza, S., Castiglioni, C. A., Kanyilmaz, A.… & Proença, J. M. (2020). A risk-consistent approach to determine EN1998 behaviour factors for lateral load resisting systems. Soil Dynamics and Earthquake Engineering, 131, 106008.

[11] Uva, G., Ciampoli, P., Leggieri, V., Nettis, A., Ruggieri, S. (2019) A Mechanical Approach for Estimating Regional Fragility Curves Of Existing Rc Buildings Stock In Puglia. In COMPDYN 2019 7th ECCOMAS Thematic Conference on Computational Methods in Structural Dynamics and Earthquake Engineering.

[12] Ruggieri S., Perrone D., Leone M., Uva G., Aiello M.A. (2020) A prioritization RVS methodology for the seismic risk assessment of RC school buildings. International Journal of Disaster Risk Reduction. Vol. 51, 101807. https://doi.org/10.1016/j.ijdrr.2020.101807

[13] Silva V., Akkar S., Baker J.W., Bazzurro P., Castro J.M., Crowley H., Dolsek M., Galasso C., Lagomarsino S., Monteiro R., Perrone D., Pitilakis K., Vamvatsikos D. (2019) Current challenges and future trends in analytical fragility and vulnerability modelling. Earthquake Spectra, DOI: 10.1193/042418EQS101O.

[14] Porter, K., Farokhnia, K., Vamvatsikos, D., and Cho, I., (2015). Guidelines for Component-Based Analytical Vulnerability Assessment of Buildings and Nonstructural Elements, Tech. Rep. 2014-10, Global Earthquake Model, Pavia, Italy.

[15] Silva. V.. Crowley. H.. Varum. H.. Pinho. R.. and Sousa. L.. (2014). Investigation of the characteristics of Portuguese regular moment-frame RC buildings and development of a vulnerability model. Bulletin of Earthquake Engineering 13. 1–36.

[16] Villar-Vega M, Silva V, Crowley H, Yepes C, Tarque N, Acevedo AB, Hube MA, Gustavo CD, Santa María H. (2017) Development of a Fragility Model for the Residential Building Stock in South America. Earthquake Spectra; 33(2): 581–604.

[17] Borzi B., Pinho R., Crowley H. (2008) Simplified Pushover-Based vulnerability analysis for large scale assessment of RC buildings. Engineering Structures, 30(3): 804-820.

[18] Jamšek. A.. & Dolšek. M. (2020). Seismic analysis of older and contemporary reinforced concrete frames with the improved fish-bone model. Engineering Structures. 212. 110514.

[19] Ruggieri S., Chatzidaki A., Vamvatsikos D., Uva G. (2021) Reduced-order models for the seismic assessment of plan-irregular low-rise moment-frame buildings. Earthquake Engineering and Structural Dynamics (submitted - under review)

[20] Ruggieri, S., & Uva, G. (2020). Accounting for the spatial variability of seismic motion in the pushover analysis of regular and irregular rc buildings in the new Italian building code. Buildings, 10(10), 177.

[21] Ruggieri S.. Porco F.. Uva G.. Vamvatsikos D. (2021) Two frugal options to assess class fragility and seismic safety for low-rise reinforced concrete school buildings in Southern Italy. Bulletin of Earthquake Engineering. DOI: 10.1007/s10518-020-01033-5.

[22] Italian National Institute of Statistics (ISTAT), 15◦ Censimento generale della popolazione e delle abitazioni (2011). Website: https://www.istat.it/it. in Italian.

[23] Greco R., Marano G., Mezzina M., Milella S., Raffaele D., Palmisano F., Porco F., Trulli I., Uva G., Il Progetto ARISTOTELES. Un’analisi Tecnico-Economica Sulle Strutture Scolastiche in Puglia (In Italian).

[24] Italian Ministry of University and Research (MIUR), Portale unico della scuol (2019) Website: https://dati.istruzione.it/ (In Italian).
[25] Vamvatsikos, D., and Cornell, C. A. (2002) Incremental dynamic analysis. Earthquake Engineering & Structural Dynamics, 2002, 31(3), 491–514.
[26] Ruiz-García, J., and Miranda, E. (2007) Probabilistic estimation of maximum inelastic displacement demands for performance-based design, Earthquake Engineering and Structural Dynamics 36, 1235–1254.
[27] Miranda E., Ruiz-Garcia J. (2002) Evaluation of approximate methods to estimate maximum inelastic displacement demands. Earthquake Engineering and Structural Dynamics. Vol. 31, No. 3, pp. 539-560.
[28] Vamvatsikos D., Cornell C.A. (2006) Direct estimation of the seismic demand and capacity of oscillators with multi-linear static pushovers through IDA. Earthq Eng Struct Dyn, 35:1097–1117.
[29] FEMA-P440A (2009) Effects of Strength and Stiffness Degradation on Seismic Response. Applied Technology Council: 201 Redwood Shores Parkway, Suite 240, Redwood City, California 94065.
[30] Lagomarsino S, Giovinazzi S. (2006) Macroseismic and mechanical models for the vulnerability and damage assessment of current buildings. Bulletin of Earthquake Engineering; 4(4): 415–443.
[31] Vamvatsikos D, Aschheim MA. (2016) Performance-based seismic design via yield frequency spectra. Earthquake Engineering and Structural Dynamics; 45(11): 1759–1778.
[32] Kohrangi, M., Bazzurro, P. & Vamvatsikos, D. Seismic risk and loss estimation for the building stock in Isfahan. Part I: exposure and vulnerability. Bull Earthquake Eng (2021). https://doi.org/10.1007/s10518-020-01036-2
[33] Moehle JP. (1992) Displacement-Based Design of RC Structures Subjected to Earthquakes. Earthquake Spectra 1992; 8(3): 403–428.
[34] Katsanos EI, Vamvatsikos D. (2017) Yield frequency spectra and seismic design of code-compatible RC structures: an illustrative example. Earthquake Engineering and Structural Dynamics; 46(11): 1727–1745.
[35] FEMA, HAZUS99 Technical Manual. Service Release 2, Federal Emergency Management Agency, Washington, D.C., USA, 2001.
[36] DM 17/01/2018, Aggiornamento delle Norme Tecniche per le Costruzioni. Gazzetta Ufficiale n. 42. del 20/02/2018. Rome. 2008. (In Italian)
[37] McKenna F. (2011) OpenSees: a framework for earthquake engineering simulation. Comput Sci Eng;13:58–66.
[38] Cornell. C. A.. Jalayer. F.. Hamburger. R. O.. and Foutch. D. (2002) Probabilistic Basis for 2000 SAC Federal Emergency Management Agency Steel Moment Frame Guidelines. Journal of Structural Engineering.